Faraday Discussions

Cite this: *Faraday Discuss.*, 2023, **241**, 448

ROYAL SOCIETY OF CHEMISTRY

PAPER

View Article Online
View Journal | View Issue

AgX-based hybrid coordination polymers: mechanochemical synthesis, structure and luminescence property characterization†

Caterina Zuffa, [a] Chiara Cappuccino, [b] Marianna Marchini, [a] Laura Contini, [a] Francesco Farinella‡[a] and Lucia Maini *[a]

Received 5th May 2022, Accepted 6th July 2022
DOI: 10.1039/d2fd00093h

Hybrid coordination polymers are interesting for their ability to converge the properties of both inorganic and organic systems in one single compound and recently attention has been focused on silver based hybrid coordination polymers due to their luminescence properties. We searched the CSD to establish the propensity of AgXL (X = Cl^-, Br^- and I^-) with L as an organic ligand to form hybrid coordination polymers. About 800 AgXL structures are deposited in the CSD, with huge structural variability: indeed, it is possible to recognize some structural preferences based on the halide nature. The formation of an inorganic polymeric unit is favoured by iodide but it is also possible with the other halides. This research continues with the synthesis of AgX (X = I^-, Br^-) based coordination polymers with 2-, 3- and 4-picolylamine (*n*-pica) as ligands. By mechanochemical synthesis five new hybrid coordination polymers and one coordination polymer have been obtained and their structures determined. While $[(AgI)(n\text{-pica})]_n$ are not luminescent, $[(AgBr)(n\text{-pica})]_n$ emit and their profile depends on the crystallinity of the sample.

Introduction

Nowadays, chemistry is increasingly directed towards the synthesis of new molecules and functional materials, which can be applied in technological, pharmaceutical, and electronic fields. The properties of materials mainly depend on their chemical nature, composition, and structure. To gain control over these features, crystal engineering has acquired significant importance.[1] The task of crystal engineering consists in assembling molecular and ionic components within a desired structure, consisting of a network of supramolecular interactions

[a]*Dipartimento di Chimica "G. Ciamician", Università di Bologna, Via F. Selmi 2, Bologna, Italy. E-mail: l.maini@unibo.it; Tel: +39 051 2099597*

[b]*Department of Chemical Science and Bernal Institute, University of Limerick, Limerick, Ireland*

† Electronic supplementary information (ESI) available. CCDC 2170412, 2170471–2170476. For ESI and crystallographic data in CIF or other electronic format see DOI: https://doi.org/10.1039/d2fd00093h

‡ F. F. is now working in Aptuit, Verona, Italy.

that bind the various units. In fact, numerous types of interactions can be established between atoms, ions, or molecules: covalent bonds, coordination bonds, Coulombic interactions, hydrogen bonds and van der Waals forces.[2,3] A combination of these interactions can also occur, and this happens, for example, in the case of coordination polymers. Coordination polymers are defined by IUPAC as "coordination compounds with repeating coordination entities extending in 1, 2 or 3 dimensions".[4,5] The ligand must be a multidentate organic molecule with at least one carbon among the donor atoms,[6] and the network must extend in at least one dimension. A particular subset of coordination polymers consists of compounds based on organic ligands and metal-oxide, -sulfide or -halide subunits. In these cases the infinite network can be due to the presence of inorganic polymeric subunits and to highlight the double organic and inorganic nature of these compounds we refer to them as hybrid coordination polymers.[7,8] This class of materials is interesting because it converges the properties of both inorganic and organic systems in one single compound,[9–11] and their utilization spans from the optoelectronic and field-transistor fields,[12] to asymmetric catalysis and enantioselective separation.[12,13] Noble metals such as Cu and Ag are particularly prone to forming hybrid coordination polymers; this is probably due to the high structural variability which depends on the different coordination geometry that such metals assume,[14] and the interaction between d^{10} cations (Cu^+, Ag^+). These interactions are defined as metallophilic and characterized by a distance between the metal centers of less than twice the van der Waals radius of the corresponding cation (Cu–Cu < 2.89 Å, Ag–Ag < 3.44 Å).[15] The noble metal coordination compounds are luminescent in the solid state and their study is oriented towards application in optoelectronics for development of OLEDs (organic light emitting diode devices).[16–19] Initially the attention was focused on $Cu_4X_4L_4$ clusters,[16] where X represents a halide while L indicates an aromatic ligand, usually of the family of pyridine and phosphine, but interesting results have also been obtained with different geometries[20] and with Cu(I)[21] hybrid coordination polymers having cuprophilic interactions.[15] In all cases, the compounds show unstructured emission bands and most of the time they show thermochromic and mechanochromic luminescence properties.[16,17] In the case of hybrid coordination polymers, the conductivity properties have been studied too.[22] Compounds and hybrid coordination polymers containing AgX are almost unexplored, but they can have argentophilic interactions, which cause a change in the emission process, leading to highly visible luminescence,[23–25] and in some cases, they show a thermochromic phenomenon directly related to the interaction between the metal centers.[26] As already said for Cu-based polymers, Ag-based compounds could also find a great application in OLEDs, because of the interesting possibility of modulating the intensities and wavelengths of emission by varying the polymer structure, the binder and the used halide.[27]

We recently published the thermochromic properties of $[(CuI)(3\text{-pica})]_n$ (ref. 21) which shows high luminescence and thermochromic behavior. Ongoing studies also revealed mechanochromic properties as observed for other CuI based compounds.[23–26] So, we expanded our research to AgX based coordination polymers to see if they had the same properties as CuX-based materials, especially related to mechanochromism.[29–31]

As happens for cuprous halides, the structures based on silver halides are generally produced by the condensation of tetrahedral units $[AgX_4]^{3-}$ by sharing

corners, sides or faces to form 0 to 3 dimensional structures which leads to a strong variability of the final inorganic units.[9,32,33] In Table 1 we report the most common inorganic units observed in structures classified according to the coordination number (μ) of the halide bound to the silver cation.

Although the variability of the AgX units is known, the frequency of the different inorganic units has not been studied yet, which prevents the possibility of designing the outcome. For this reason, we explored the CSD (Cambridge Structural Database)[34] following a data mining and KDD (Knowledge Discovery in Databases) approach. If the goal of data mining is purely statistical and aimed in search of mathematical relationships between data, KDD sets itself the aim of interpreting these relationships to extract knowledge.[35,36] As expected, the halides have a different propensity for μ coordination which influences the final structures and the presence of argentophilic interactions. The argentophilic interaction was evaluated only by the distance criterion between the metal atoms as already mentioned,[23,37–39] but we are conscious that other criteria should be used to validate the interactions such as theoretical-computational analysis[38,40–46] and vibrational spectroscopy.[47–52]

Encouraged by the KDD results, which confirmed the similarity of CuX and AgX compounds and the possibility of obtaining structures with similar nuclearity, we proceeded with the synthesis of AgI and AgBr-based compounds. From this point of view, the main problem is the poor solubility of AgI and AgBr (K_{sp} =

Table 1 Various examples of discrete and infinite silver-halide inorganic units[33]

Coordination number	Inorganic discrete unit	Inorganic polymeric unit
μ^1	Ag–X	—
	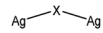 Single bridge	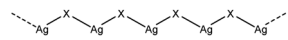 Single chain
μ^2	 Double bridge (dimer)	
	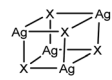 Cubane	
μ^3	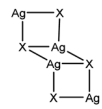 Staircase	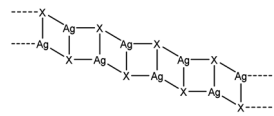 Double chain
	 Trigonal bipyramid	

8.52×10^{-17}, 5.35×10^{-13} respectively[53]) in most common solvents and also the coordination power of acetonitrile is insufficient to dissolve the inorganic salt which prevented us from following the reaction in the same solutions as the CuX compounds. In the search for a more sustainable eco-friendly approach to synthetic procedures and to overcome this difficulty, we practiced solvent-less methods, such as mechanochemical reactions, which have been demonstrated to be an attractive and viable alternative especially for the synthesis of CuX coordination polymers.[28,54–56] We have explored the reactions of AgX ($X = I^-$, Br^-) with three isomers, 2-, 3- and 4-picolylamine (pica); the ligands are liquid and act both as a reagent and as a solvent. The reactions were performed by ball milling, by slurry to increase the crystallinity or by simple contact of the two reagents; the latter method took about fourteen days but allowed the formation of crystals suitable for crystal structure determination. Furthermore, we studied the effect of the mechanical process on the luminescence properties. We obtained five new hybrid coordination polymers $[(AgI)(n\text{-pica})]_n$ ($n = 2, 3, 4$) and $[(AgBr)(n\text{-pica})]_n$ ($n = 2, 3$) and one coordination polymer $[(AgBr)(4\text{-pica})]_n$. While AgI-based compounds present the desired double chain and argentophilic interactions as expected from KDD, these compounds did not show any luminescence properties. For this reason, we expanded the study to AgBr(*n*-pica) coordination polymers which present a strong variety with respect to the inorganic nuclearity, as suggested by KDD, and they are luminescent. In particular $[(AgBr)(2\text{-pica})]_n$ is mechanochromic, and the emission is promoted by the grinding process. Further studies will also be accomplished on $[(AgBr)(4\text{-pica})]_n$ whose emission profile is quite different depending on the synthetic process and crystallinity.

Materials and methods

Knowledge discovery in databases

We checked the probability of obtaining AgX-based hybrid coordination polymers using the ConQuest software.[57] We examined the role of the halide in compounds AgXL – where X = Cl, Br, or I and L is an organic ligand with the atom binding directly to silver being N, P, As, O, S, or Se – deposited in the Cambridge Structural Database (CSD),[34] version 5.43 released in November 2021. The Knowledge Discovery in Databases (KDD) approach was used, to obtain general indications on the behavior of the different halides and their influence on the final geometry of the compounds. Thanks to the possibility of investigating the Ag–Ag distance values in each structure, it was possible to identify the presence of argentophilic interactions, based on the distance criterion.[38]

Synthesis

All the reagents were purchased from Sigma-Aldrich. AgI and AgBr were solids and all the ligands (2-, 3- and 4-picolylamine, from now on called 2-, 3- and 4-pica) were in liquid form. To minimise the granularity of the AgX salts, and therefore maximise the contact surface of the reagents, AgI and AgBr were recrystallized by dissolving the salt in a saturated solution of KI (KBr in the case of AgBr) and then quickly precipitated by adding pure water to the solution. All the reactions must be performed in a vessel covered with aluminum foil to prevent degradation because the silver halide reagents and the products obtained are photosensitive.

Synthesis of $[(AgI)(n\text{-pica})]_n$

Contact reaction. 1 mmol of AgI (0.235 g) was covered with 1 mmol of *n*-pica (0.1 mL) in a glass vessel, mixed a little with a spatula and kept still in the dark for at least 14 days. We obtained needle-shape single crystals of $[(AgI)(3\text{-pica})]_n$ and $[(AgI)(4\text{-pica})]_n$ and a crystalline powder of $[(AgI)(2\text{-pica})]_n$, not suitable for SCXRD analysis.

Mechanochemical reaction. 1 mmol of AgI (0.235 g) and 1 mmol of *n*-pica (0.1 mL) were placed in a 10 mL agate ball-milling jar. The agate sphere used had a diameter of 5 mm. We milled our reactants at 20 rpm (0.33 Hz) for 120 minutes. The crystalline powders obtained were analyzed by XRPD.

Slurry. 1 mmol of AgI (0.235 g) and 1 mmol of *n*-pica (0.1 mL) were placed in a glass vessel with 1.5 mL of acetonitrile and the slurry was stirred in the dark for 24 hours. We obtained crystalline powders without unreacted AgI.

Synthesis of $[(AgBr)(n\text{-pica})]_n$

Contact reaction. 1 mmol of AgBr (0.188 g) was covered with 1 mmol of *n*-pica (0.1 mL) in a glass vessel, mixed a little with a spatula and kept still in the dark for at least 14 days. We obtained needle-shape single crystals of $[(AgBr)(2\text{-pica})]_n$ and $[(AgBr)(3\text{-pica})]_n$ and a crystalline powder of $[(AgBr)(4\text{-pica})]_n$, not suitable for SCXRD analysis.

Mechanochemical reaction. 1 mmol of AgBr (0.188 g) and 1 mmol of *n*-pica (0.1 mL) were placed in a 10 mL agate ball-milling jar. The agate sphere used had a diameter of 5 mm. We milled our reactants at 20 rpm (0.33 Hz) for 120 minutes. The crystalline powders obtained were analyzed by XRPD.

Slurry. 1 mmol of AgBr (0.188 g) and 1 mmol of *n*-pica (0.1 mL) were placed in a glass vessel with 1.5 mL of acetonitrile and the slurry was stirred in the dark for 24 hours. We obtained crystalline powders without unreacted AgBr.

After all the reactions, all the obtained products must be washed with acetonitrile.

The crystallographic data were collected with both single crystal and powder X-ray diffractometers, depending on the compound analyzed.

Structure determination by single crystal and powder X-ray diffraction

The single crystal data of $[(AgI)(3\text{-pica})]_n$, $[(AgI)(4\text{-pica})]_n$, $[(AgBr)(2\text{-pica})]_n$ and $[(AgBr)(3\text{-pica})]_n$ were collected at room temperature on an Oxford Xcalibur using Mo-Kα radiation, equipped with a graphite monochromator and a CCD Sapphire detector. Crystal data details are summarized in Table 2 (see also Tables 3 and 4 in the ESI†). The SHELXT[58] and SHELXL[59] algorithms were used for the solution and refinement of the structures based on F^2. All the atoms, excluding the hydrogens, were refined anisotropically. Hydrogen atoms have been added to the theoretical positions.

The structures of $[(AgI)(2\text{-pica})]_n$ and $[(AgBr)(4\text{-pica})]_n$ were solved by X-ray powder diffraction. The powder data were obtained on a Panalytical X'Pert PRO using Cu-Kα radiation, endowed with micro-focusing, a pixel detector and a capillary holder. The sample was loaded in a 0.5 mm glass capillary. The analysis was carried out in transmission mode and data were collected in the 2θ range of 5–70°, with a 0.02 rad soller slit, a $\frac{1}{2}^\circ$ divergence slit and a $\frac{1}{2}^\circ$ antiscatter slit. Six consecutive repetitions of the same measurement were collected and merged to obtain an optimal ratio between the signal and the noise.

Table 2 Crystal data and structure refinement for $[(AgI)(n\text{-pica})]_n$ coordination polymers

	$[(AgI)(2\text{-pica})]_n$	$[(AgI)(3\text{-pica})]_n$	$[(AgI)(4\text{-pica})]_n$
Empirical formula	$C_6H_8AgIN_2$	$C_6H_8AgIN_2$	$C_6H_8AgIN_2$
Formula weight (g mol^{-1})	342.91	342.91	342.91
T (K)	293	293	293
Wavelength (Å)	1.535	0.71073	0.71073
Crystal system	Triclinic	Monoclinic	Monoclinic
Space group	$P\bar{1}$	$P2_1/c$	$P2_1/c$
a (Å)	4.579	16.9162(7)	4.4664(3)
b (Å)	10.323	4.5682(2)	19.2155(11)
c (Å)	10.263	22.7197(8)	10.5788(6)
α (°)	112.54	90	90
β (°)	83.86	90.447(4)	96.346(5)
γ (°)	85.59	90	90
V (Å^3)	442	1755.65(12)	902.35(9)
Z, Z'	2, 1	4, 1	4, 1
Goodness-of-fit on F^2	2.036	1.041	1.051
$R1$ $[I > 2\sigma(I)]$	0.028	0.0596	0.0486
w$R2$ (all data)	0.037	0.1351	0.0837

The analysis of the powder data was performed using the software TOPAS 6;[60] a Chebyshev function and a pseudo-Voigt (TCHZ type) were used to fit the background and the peak shape, respectively. The powders were indexed with the cells reported in Tables 2 and 3. The structure was determined by simulated annealing and refined by the Rietveld method. All the hydrogen atoms were fixed in calculated positions. CCDC 2170471–2170476 contain the supplementary crystallographic data for this paper. The data can be obtained free of charge from

Table 3 Crystal data and structure refinement for $[(AgBr)(n\text{-pica})]_n$ coordination polymers

	$[(AgBr)(2\text{-pica})]_n$	$[(AgBr)(3\text{-pica})]_n$	$[(AgBr)(4\text{-pica})]_n$
Empirical formula	$C_6H_8AgBrN_2$	$C_6H_8AgBrN_2$	$C_6H_8AgBrN_2$
Formula weight (g mol^{-1})	295.915	295.915	295.915
T (K)	293	293	293
Wavelength (Å)	0.71073	0.71073	1.535
Crystal system	Triclinic	Monoclinic	Monoclinic
Space group	$P\bar{1}$	$P2_1/c$	$P2_1/c$
a (Å)	4.3871(5)	9.4518(6)	6.316
b (Å)	10.1081(12)	6.1880(3)	7.365
c (Å)	10.2510(18)	14.3981(9)	17.769
α (°)	113.498(14)	90	90
β (°)	97.081(12)	105.712(6)	81.08
γ (°)	93.535(9)	90	90
V (Å^3)	410.63(11)	810.64(8)	816
Z, Z'	2, 1	4, 1	4, 1
Goodness-of-fit on F^2	0.983	1.041	1.301
$R1$ $[I > 2\sigma(I)]$	0.0448	0.0419	0.0285
w$R2$ (all data)	0.0854	0.0852	0.0358

the Cambridge Crystallographic Data Centre *via* **https://www.ccdc.cam.ac.uk/structures**.

The graphical representations of the structures were displayed with the MERCURY program.[61]

Photochemical measurements

We acquired reflectance spectra of the samples in the solid state with a PerkinElmer Lambda 950 UV/vis/NIR spectrophotometer equipped with a 100 mm integrating sphere and converted them into absorption spectra using the Kubelka–Munk function.[62,63] We also collected the emission spectra of the compounds in the solid state, in front-face mode with an Edinburgh FLS920 fluorimeter equipped with a Peltier-cooled Hamamatsu R928 PMT (280–850 nm), and corrected for the wavelength-dependent phototube response.

Results and discussion

Knowledge discovery in databases

The high structural variability of silver compounds prompted us to study the role of the halide in determining the geometry of AgXL compounds. Ag^+ is a widely used metal ion acceptor in coordination chemistry and features a flexible coordination sphere. This flexile nature determines the capability of adopting variable coordination numbers starting from one up to values above 8. This variability is mainly due to the lack of stereochemical preference that arises from the d^{10} configuration, together with the weakness of the silver–ligand bonds.[64] To quantify such structural variability, we searched the database for all the deposited structures containing coordinated Ag (21 433 hits) and evaluated the distribution of the possible coordination numbers. We compared the results with the same distribution for the subset_AgXL (791 hits) which contains only structures with the silver atom bound to the halide. Fig. 1 shows how the presence of the halide significantly reduces the variability in Ag(I) coordination: in the subset_AgXL 81% of the deposited structures present a four-coordinate Ag^+, whereas the same coordination represents only 45% of the subset containing all the compounds containing Ag^+ deposited in the CSD.

The structure variability observed in our compounds is thus mostly ascribable to the role of the halide ion, which was then studied in more depth. The halide can act as a bridging ligand connecting two or more Ag(I) ions simultaneously. We quantified such structural variability by determining the coordination number of the halide in each structure of the subset_AgXL (see Table 4).

The distribution shows that all halides have a high tendency to act as bridging ligands between two or more Ag(I) ions and the tendency to give structures with μ^1 halides decreases on passing from Cl to Br to I, 38%, 28% and 17% respectively (see Table 4). The skill of the halide to act as a bridging ligand favors the variability in the formation of different inorganic geometries as shown in Table 1.

Nevertheless, the halide coordination propensity is quite spread out and only bromide clearly favours μ^2 coordination (45%, Table 4) which is associated with single and double bridges and, while for the first geometry it is easy to obtain infinite repetition (*i.e.*, single chain), for the second one it is rarer and this geometry is usually related to the formation of the dimer. In particular for Br-μ^2

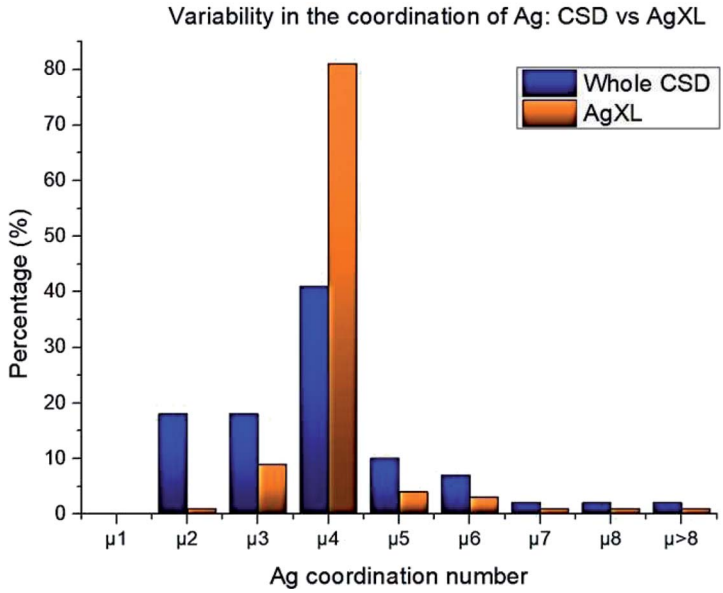

Fig. 1 Statistical distribution of silver coordination number both in the whole CSD database and in our subset_AgXL.

Table 4 Percentage distribution of the structures formed by each halide depending on the number of Ag(I) atoms coordinated by the halide X (X = Br, Cl, I)

	%X-μ^1	%X-μ^2	%X-μ^3	%X-$\mu^{>3}$
Chlorides	38	34	18	10
Bromides	28	45	19	9
Iodides	17	34	38	12

86% of the structures have a dimeric inorganic unit, which prevents the formation of hybrid coordination polymers. The formation of infinite inorganic units and hence of hybrid coordination polymers is favoured in the case of X-μ^3 as shown in Table 5.

Our interest is focused on the possibility of obtaining hybrid coordination polymers hence we divided the subset_AgXL (with X = Cl, Br, I) into structures containing discrete and polymeric inorganic units. It is worth noting that

Table 5 The different percentages of structures that display an inorganic discrete unit and infinite repetition of the inorganic unit for each coordination

	Inorganic discrete unit	Inorganic polymeric unit
X-μ^1	100	0
X-μ^2	91	9
X-μ^3	64	36
X-$\mu^{>3}$	62	38

structures containing an inorganic discrete unit can also be polymeric but, in this case, the infinite repetition only depends on the coordination capability of the organic ligand, which has not been evaluated in this paper.

As shown in Table 6, most of the structures display an inorganic discrete unit, although the percentage of inorganic polymeric units is significantly higher for iodides. However, the geometry of the inorganic motif in these two subclasses is significantly different for the three halides and this is strongly influenced by the different propensity for coordination of the three, as described earlier. To understand this aspect, we classified both inorganic discrete and polymeric units depending on the μ number of the halide ligand (see Fig. 2).

Chloride and bromide have a high tendency to form inorganic discrete units (88% and 86% respectively), even if the coordination is quite different. Chloride prefers μ^1 (45%) while bromide clearly prefers μ^2 (48%). On the other hand, iodide does not show any preference in coordination but it shows a higher percentage of μ^3 probably due to the higher atomic radius.

In hybrid coordination polymers, chloride does not show any preference in the μ-number while bromide and in particular iodide prefer μ^3 coordination mainly due to the formation of a double chain as also observed in our compounds (see later).

Lastly, iodide is the halide displaying the highest tendency to form hybrid coordination polymers (23%) which is correlated to the larger tendency of I to form μ^3 and $\mu^{>3}$ structures (see Table 6). We have observed that these types of coordination promote the formation of hybrid coordination polymers as shown in Table 5.

Table 6 The different percentages (for each halide) of structures that display an inorganic discrete unit and infinite repetition of the inorganic unit

	Inorganic discrete unit	Inorganic polymeric unit
Chlorides	88	12
Bromides	86	14
Iodides	77	23

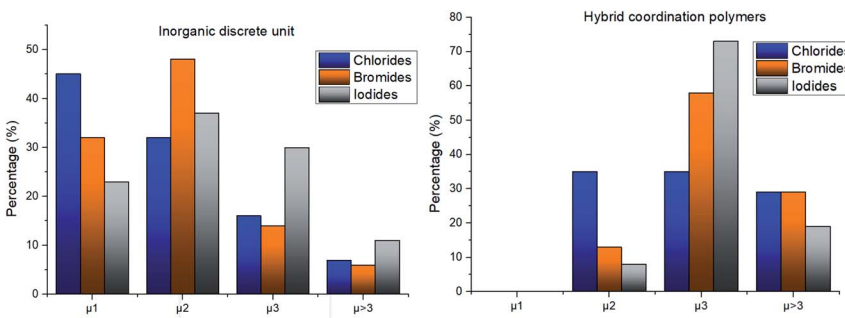

Fig. 2 Percentage of the coordination number of the different halides in the structures that have inorganic discrete units and percentage of the coordination number of the different halides in the hybrid coordination polymers.

Argentophilic interactions

We evaluated the presence of argentophilic interactions in the structures present in the AgXL_subset, based on the distance criterion and by searching for the structures displaying a short contact between Ag(I) centres of less than 3.44 Å, accounting for both intermolecular and intramolecular contacts. We observed that 47% of the structures present in our subset satisfy the distance criterion: a percentage larger than the one obtained considering all the structures containing Ag(I) deposited in the database (31%). We can ascribe this result to the high number of AgXL structures displaying a bridging halide, which supports the metallophilic interactions. It is worth noting that AgClL compounds are slightly less prone to having argentophilic interactions (36% of the AgCl-based structures contain argentophilic interactions) with respect to AgBrL (46%) and AgIL (67%).

AgI-based coordination polymers

KDD clearly indicates that the percentage of hybrid coordination polymers for the AgXL compounds is low but their formation is still possible and in particular, iodide promotes the formation of inorganic polymeric units. As observed for CuI, the mechanochemical reaction favors the formation of the hybrid coordination polymer[65] and at the same time, can overcome the problem of the solubility of the AgX salts. In fact, solid AgI promptly reacts with the organic ligands by ball milling and $[(AgI)(n\text{-pica})]_n$ were obtained in a couple of hours. To obtain single crystals the reactions were performed by simply leaving the AgI powder embedded in the liquid ligand for at least 14 days. Reactions in solution or solvothermal reactions failed, due to the low solubility of the AgI. Reaction by slurry increased the crystallinity of the product but no other crystal phases have been observed.

$[(AgI)(n\text{-pica})]_n$. $[(AgI)(n\text{-pica})]_n$ compounds can be easily obtained by mechanochemical reactions; in the case of $[(AgI)(3\text{-pica})]_n$ and $[(AgI)(4\text{-pica})]_n$, needle-shape crystals were synthesized by contact reactions and their structures were solved by single crystal X-ray diffraction. In the case of $[(AgI)(2\text{-pica})]_n$ the structure was determined by X-ray powder diffraction. The asymmetric unit for $[(AgI)(2\text{-pica})]_n$ and $[(AgI)(4\text{-pica})]_n$ is composed of one silver atom and one ligand coordinating the metal by the nitrogen of the amino group and the iodide. In the $[(AgI)(3\text{-pica})]_n$ structure, the asymmetric unit is made of two independent AgI–3-pica moieties. In all compounds the structures are characterized by a double chain of AgI where the tetrahedral Ag coordinates three iodide atoms and the ligand, forming infinite ribbons as shown in Fig. 3. It is quite interesting to note that the picolylamine, although it is bidentate, never bridges two silver atoms as observed in the CuI-based coordination polymers,[21,28] and the aromatic N atom forms hydrogen bonds with the amino group of a contiguous ligand molecule. The different structures obtained with silver and copper halides could be due to the different synthesis, however the mechanochemical reaction of CuI with 3-pica was prevented by the instantaneous oxidation of Cu(I) in the presence of the basic ligand, while it was not possible to perform the reaction in solution in the case of the silver halide.

In $[(AgI)(2\text{-pica})]_n$ the hydrogen bonds link ligands belonging to the same chain and the overall crystal packing can be described as ribbons running parallel to each other in a layered structure. In $[(AgI)(3\text{-pica})]_n$ and $[(AgI)(4\text{-pica})]_n$ hydrogen bonds are formed between ligands belonging to different ribbons and

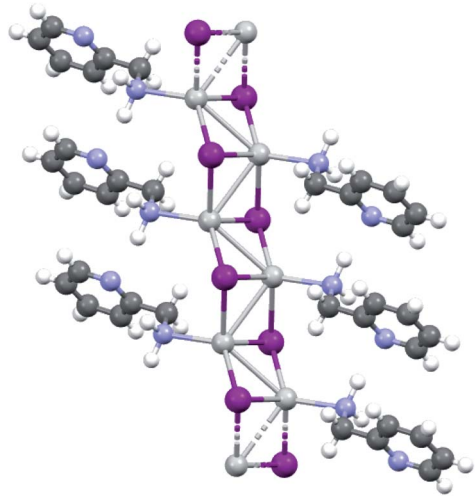

Fig. 3 AgI double chain present in the $[(AgI)(2\text{-pica})]_n$ structure. The silver atom (grey) coordinates the N of the amino group of the ligand and 3 iodide atoms (purple). The argentophilic interactions are highlighted.

this promotes the formation of herringbone motifs. In all hybrid coordination polymers, the Ag–Ag distances are shorter than 3.44 Å which suggests the presence of argentophilic interactions (see Table 7 for distances between two contiguous Ag^+ cations) (Fig. 4).

As previously mentioned, we achieved what was predicted by the KDD approach. In the $[(AgI)(n\text{-pica})]_n$ structures I^- has μ^3 coordination which promoted the formation of the inorganic double chain and the argentophilic interactions. Despite this successful design, the products are not luminescent, and for this reason we explored the possibilities of hybrid coordination compounds based on silver bromide.

AgBr-based coordination polymers

The KDD results show that bromide prefers μ^2 coordination and hence should favor the formation of an inorganic discrete unit. However, in our results $[(AgBr)(n\text{-pica})]_n$ presents a high structure variability and a propensity for hybrid

Table 7 Distances between two contiguous Ag^+ cations

Compound	Ag–Ag distance (Å)
$[(AgI)(2\text{-pica})]_n$	3.136
	3.179
$[(AgI)(3\text{-pica})]_n$	3.219
	3.037
	3.329
$[(AgI)(4\text{-pica})]_n$	3.128
	2.942

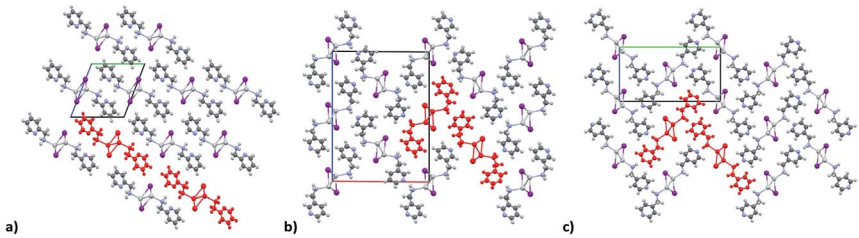

Fig. 4 (a) $[(AgI)(2\text{-pica})]_n$ packing along the *a*-axis, the ribbons are all parallel (highlighted in red); (b) $[(AgI)(3\text{-pica})]_n$ packing along the *b*-axis, the slightly distorted herringbone structure is clear (see the molecules highlighted in red); (c) $[(AgI)(4\text{-pica})]_n$ packing along the *a*-axis, the herringbone structure is visible (see the molecules highlighted in red). Cell axis colour: *a* is red, *b* is green and *c* is blue.

coordination polymers. Indeed, the dimer is observed in $[(AgBr)(4\text{-pica})]_n$, but $[(AgBr)(2\text{-pica})]_n$ is characterized by the presence of a double chain common for hybrid coordination polymers based on AgI while $[(AgBr)(3\text{-pica})]_n$ has a single chain which is mainly observed in hybrid coordination polymers based on AgCl.

$[(AgBr)(2\text{-pica})]_n$. The crystalline structure of $[(AgBr)(2\text{-pica})]_n$ was determined by SCXRD on a colorless, needle-like crystal obtained through contact reaction. The packing is isomorphous to the structure of $[(AgI)(2\text{-pica})]_n$ (Fig. 5). The structure is characterized by a double chain of AgBr with Ag–Ag distances of 3.199 Å and 3.299 Å, a little bit longer than those observed in the isomorphic compound. μ^3 coordination for Br^- is only present in 19% of structures (Table 4), but for AgBr-based hybrid coordination polymers the double chain is not so uncommon (Fig. 2).

$[(AgBr)(3\text{-pica})]_n$. The crystalline structure of $[(AgBr)(3\text{-pica})]_n$ was solved by SCXRD on a colorless, needle-like crystal synthesized *via* contact reaction. The structure is characterized by a single chain formed by alternating silver and bromine atoms (Fig. 6a). The 3-pica bridges these chains by coordinating the silver cations with both pyridine and amino nitrogen. This generates infinite two-dimensional planes where the two propagation directions are due to the

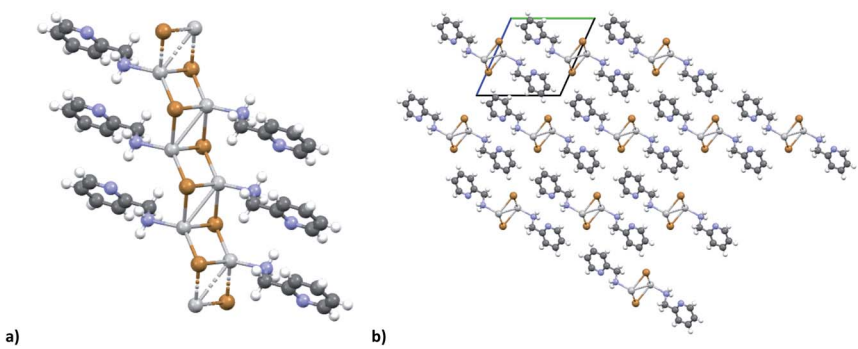

Fig. 5 (a) AgBr double chain (isomorphic to $[(AgI)(2\text{-pica})]_n$) with the argentophilic interactions highlighted; (b) packing along the *a*-axis, the structure is colored according to symmetry equivalence. Cell axis colour: *a* is red, *b* is green and *c* is blue.

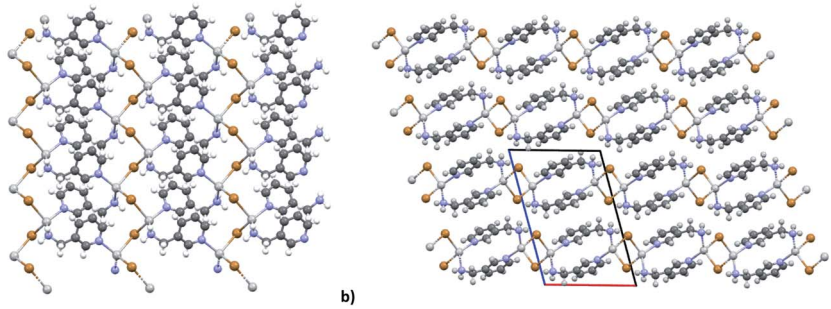

Fig. 6 (a) Single chain of AgBr; (b) packing along the *b*-axis. All the "chains" are parallel; they are layers. Cell axis colour: *a* is red, *b* is green and *c* is blue.

alternating of the organic ligand and the metal node typical of coordination polymers, and the infinite inorganic chain. Due to the type of packing, Ag–Ag interactions cannot be present (Fig. 6a and b). $[(AgBr)(3\text{-pica})]_n$ does not show any similarity to the corresponding AgI-based structure; its structure was not predicted based on KDD. As already said bromide prefers μ^2 coordination to form discrete dimers (Table 4), but in $[(AgBr)(3\text{-pica})]_n$ the μ^2 coordination leads to the formation of a single chain which is very uncommon (Table 6 and Fig. 2) for this halide, but common for chloride.

$[(AgBr)(4\text{-pica})]_n$. The crystalline structure of $[(AgBr)(4\text{-pica})]_n$ was determined by PXRD on a crystalline powder obtained by ball milling. The structure has Ag cations, with the typical tetrahedral coordination, bonded to two Br^- anions forming a dimer and two 4-pica ligands, which in turn bridge to another inorganic dimer each (Fig. 7). The structure is a two-dimensional coordination polymer based on parallel corrugated layers. The dimer allows a short Ag–Ag contact, 3.198 Å, consistent with an argentophilic interaction. As observed before, the packing found for $[(AgBr)(4\text{-pica})]_n$ turns out to be different from the equivalent synthesized with AgI, which always presents a double chain structure, but it adopts the dimer as an inorganic unit which is the most common for AgBrL compounds as discussed in the previous section.

Luminescence properties

$[(AgI)(n\text{-pica})]_n$ are not luminescent regardless of the synthetic procedure or the temperature; in contrast $[(AgBr)(n\text{-pica})]_n$ are emissive and their luminescence properties have been investigated in the solid state.

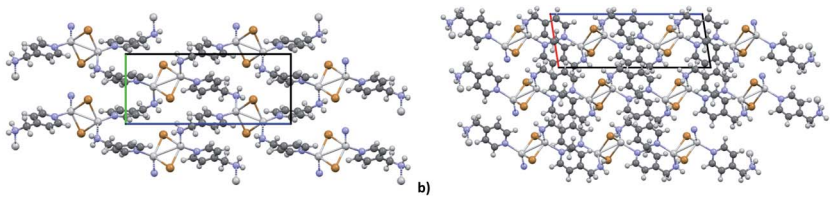

Fig. 7 (a) Packing along the *a*-axis; (b) packing along the *b*-axis. Cell axis colour: *a* is red, *b* is green and *c* is blue.

The $[(AgBr)(n\text{-pica})]_n$ compounds obtained by mechanochemical reactions absorb in the UV region and emit in the blue-green region, with a maximum around 470 nm when the ligand is 2-picolylamine, and 500 nm with both 3- and 4-picolylamine (Fig. 8). Interestingly, when $[(AgBr)(2\text{-pica})]_n$ is obtained by slurry experiment, and hence it is more crystalline, it is no longer emissive, but the emission can be recovered by manual grinding of the powder.

Conversely, $[(AgBr)(3\text{-pica})]_n$ shows a comparable behavior for the samples obtained by mechanochemical reaction and slurry even though they present a different crystallinity.

The emission spectrum of $[(AgBr)(4\text{-pica})]_n$ synthesized from slurry shows different features with respect to the sample obtained from ball milling (Fig. 9).

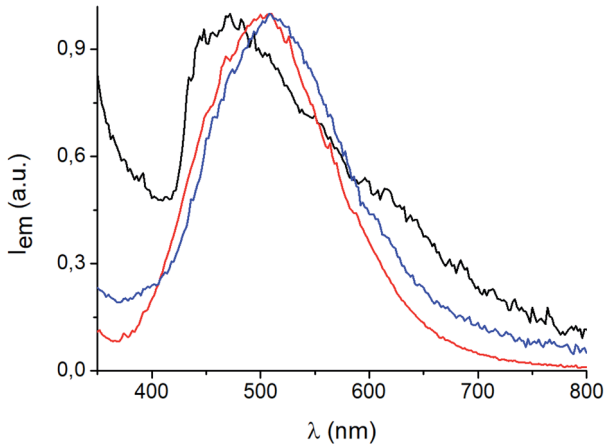

Fig. 8 Solid state emission spectra of $[(AgBr)(2\text{-pica})]_n$ (black line), $[(AgBr)(3\text{-pica})]_n$ (red line) and $[(AgBr)(4\text{-pica})]_n$ (blue line) at 298 K, $\lambda_{exc} = 300$ nm. These compounds have been obtained by mechanochemical reaction.

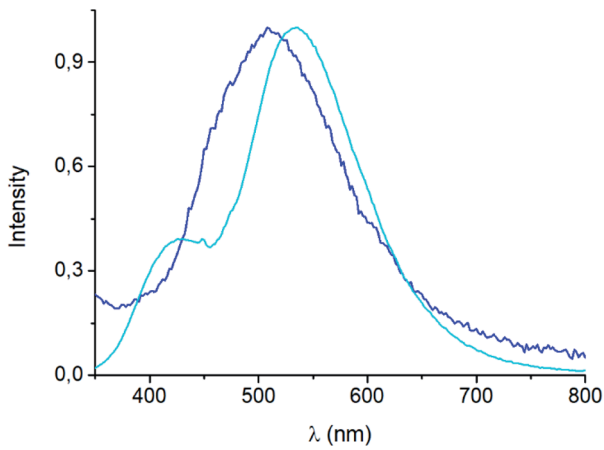

Fig. 9 Solid state emission spectra of mechanochemical (blue line) and slurry (light blue line) $[(AgBr)(4\text{-pica})]_n$ at 298 K, $\lambda_{exc} = 300$ nm.

Indeed, the maximum is now centered at 530 nm and a shoulder appears at 430 nm; the synthetic path, thus, could be crucial for the photophysical properties of these compounds.

Moving from room temperature to 77 K, no significant difference was observed in the luminescence properties of the coordination polymers obtained with mechanochemistry and slurry (see the ESI† for more details). The red-shift of the $[(AgBr)(3\text{-pica})]_n$ emission maximum at 77 K when the coordination polymer is obtained from slurry is worthy of attention.

Conclusions

Our interest in d^{10} hybrid coordination polymers prompted us to study the structure based on the silver halide and the isomers of picolylamine. Initially we performed a KDD study based on the structures deposited in the CSD to know if it was possible to obtain AgX-based hybrid coordination polymers, thinking they would have similar photochemical properties to CuX-based compounds.

The AgXL materials show a high structural variability, due to the μ^n coordination skill of the halides. The structures span from discrete to polymeric inorganic units. Although the discrete units are always preferred (see Table 6), their structures are different depending on the nature of the halide. As expected, chloride slightly prefers μ^1 coordination, while bromide prefers μ^2 coordination associated with the dimer, while iodide slightly prefers μ^3 coordination associated with the cubane. Surprisingly, in our studies 83% of $[(AgX)(n\text{-pica})]_n$ are hybrid coordination polymers, which is a dramatically higher percentage than that observed in the CSD research (16%). We cannot exclude that the data in the CSD could be biased by the synthetic procedure. Up to now the reactions in solution have been privileged, and the low solubility of the AgX salts prevents the formation of the product, and thus explains the reduced number of structures in the database. Moreover, the reactions in solution usually favor the formation of low nuclearity compounds, in contrast to the reactions in the solid state, and this is in line with what is observed in $[(AgX)(n\text{-pica})]_n$ compounds.

All the $[(AgX)(n\text{-pica})]_n$ have been obtained by ball milling, confirming the effectiveness of mechanochemical reactions as well as their sustainability. Other synthetic procedures were explored, mainly in the solid state, to obtain single crystals for structure determination; in particular the liquid nature of the ligands allowed the formation of single crystals of the products by simple contact of the reagents.

In the case of $[(AgI)(n\text{-pica})]_n$ the structures are characterized by the presence of I^- μ^3 coordination which allows the formation of AgI double chains and argentophilic interactions, while the ligand coordinates the silver atoms only with the nitrogen of the amino group. The structures obtained fulfilled the desired features (inorganic polymeric unit and metallophilic interactions), but the compounds are unexpectedly not emissive.

In the case of AgBr the structures are characterized by a high variability: Br^- is μ^3 in $[(AgBr)(2\text{-pica})]_n$ and the structure is isomorphic with the iodide analogue, Br^- is μ^2 in $[(AgBr)(3\text{-pica})]_n$ with the formation of Ag–Br single chains without argentophilic interactions and finally Br^- is μ^2 in $[(AgBr)(4\text{-pica})]_n$ with the formation of discrete dimers, quite common for AgBrL compounds. All these compounds are luminescent: $[(AgBr)(2\text{-pica})]_n$ can be described as

mechanochromic since the emission is triggered by grinding. The emission profile of $[(AgBr)(3\text{-pica})]_n$ does not change upon grinding or decreasing the temperature; finally $[(AgBr)(4\text{-pica})]_n$ presents different emission profiles depending on the crystallinity of the samples. Their photophysical properties could be related to the inorganic unit and the effect of the grinding on the structure but further studies should be done.

Author contributions

All authors have given approval to the final version of the manuscript. C. C. and F. F. performed the investigation and experimental part and structure determination. C. Z. and M. M. performed the investigation and luminescence characterization and wrote the manuscript. L. C. carried out the CSD investigation and data mining. L. M. carried out conceptualization, supervision of the work, and writing and reviewing of the manuscript.

Conflicts of interest

There are no conflicts to declare.

Acknowledgements

The authors are grateful to Dr Barbara Ventura of ISOF-CNR (Bologna) and Dr Katia Rubini (University of Bologna) for the discussion.

Notes and references

1 S. J. Maginn, *J. Appl. Crystallogr.*, 1991, **24**, 265.
2 D. Braga, F. Grepioni and G. R. Desiraju, *Chem. Rev.*, 1998, **98**, 1375–1405.
3 D. Braga, *Chem. Commun.*, 2003, **3**, 2751–2754.
4 S. R. Batten, N. R. Champness, X. M. Chen, J. Garcia-Martinez, S. Kitagawa, L. Öhrström, M. O'Keeffe, M. P. Suh and J. Reedijk, *Pure Appl. Chem.*, 2013, **85**, 1715–1724.
5 S. R. Batten, N. R. Champness, X. M. Chen, J. Garcia-Martinez, S. Kitagawa, L. Öhrström, M. O'Keeffe, M. P. Suh and J. Reedijk, *CrystEngComm*, 2012, **14**, 3001–3004.
6 J. N. Moorthy and J. J. Vittal, *J. Mol. Struct.*, 2006, **796**, 1.
7 C. Janiak, *Dalton Trans.*, 2003, **3**, 2781–2804.
8 C. Slabbert and M. Rademeyer, *Coord. Chem. Rev.*, 2015, **288**, 18–49.
9 A. Chen, S. Meng, J. Zhang and C. Zhang, *Inorg. Chem. Commun.*, 2013, **35**, 276–280.
10 G. E. Wang, G. Xu, M. S. Wang, J. Sun, Z. N. Xu, G. C. Guo and J. S. Huang, *J. Mater. Chem.*, 2012, **22**, 16742–16744.
11 H. H. Li, Z. R. Chen, L. C. Cheng, M. Feng, H. D. Zheng and J. Q. Li, *Dalton Trans.*, 2009, 4888–4895.
12 C. R. Kagan, D. B. Mitzi and C. D. Dimitrakopoulos, *Science*, 1999, **286**, 945–947.
13 M. Hong, *Cryst. Growth Des.*, 2007, **7**, 10–14.

14 D. Venkataraman, Y. Du, S. R. Wilson, K. A. Hirsch, P. Zhang and J. S. Moore, *J. Chem. Educ.*, 1997, **74**, 915–918.
15 N. V. S. Harisomayajula, S. Makovetskyi and Y. C. Tsai, *Chem.–Eur. J.*, 2019, **25**, 8936–8954.
16 C. K. Ryu, K. R. Kyle and P. C. Ford, *Inorg. Chem.*, 1991, **30**, 3982–3986.
17 P. C. Ford and A. Vogler, *Acc. Chem. Res.*, 1993, **26**, 220–226.
18 F. De Angelis, S. Fantacci, A. Sgamellotti, E. Cariati, R. Ugo and P. C. Ford, *Inorg. Chem.*, 2006, **45**, 10576–10584.
19 M. Wallesch, D. Volz, D. M. Zink, U. Schepers, M. Nieger, T. Baumann and S. Bräse, *Chem.–Eur. J.*, 2014, **20**, 6578–6590.
20 A. M. Wheaton, I. A. Guzei and J. F. Berry, *Acta Crystallogr., Sect. E: Crystallogr. Commun.*, 2020, **76**, 1336–1344.
21 F. Farinella, L. Maini, P. P. Mazzeo, V. Fattori, F. Monti and D. Braga, *Dalton Trans.*, 2016, **45**, 17939–17947.
22 H. N. Wang, X. Meng, L. Z. Dong, Y. Chen, S. L. Li and Y. Q. Lan, *J. Mater. Chem. A*, 2019, **7**, 24059–24091.
23 H. Schmidbaur and A. Schier, *Angew. Chem., Int. Ed.*, 2015, **54**, 746–784.
24 T. Kuwahara, H. Ohtsu and K. Tsuge, *Inorg. Chem.*, 2021, **60**, 1299–1304.
25 R. M. Almotawa, G. Aljomaih, D. V. Trujillo, V. N. Nesterov and M. A. Rawashdeh-Omary, *Inorg. Chem.*, 2018, **57**, 9962–9976.
26 M. Dosen, Y. Kawada, S. Shibata, K. Tsuge, Y. Sasaki, A. Kobayashi, M. Kato, S. Ishizaka and N. Kitamura, *Inorg. Chem.*, 2019, **58**, 8419–8431.
27 X. Li, C. Ding, X. Li, Y. Ding, S. W. Ng and Y. Xie, *Cryst. Growth Des.*, 2012, **12**, 3465–3473.
28 C. Cappuccino, F. Farinella, D. Braga and L. Maini, *Cryst. Growth Des.*, 2019, **19**, 4395–4403.
29 S. Perruchas, X. F. L. Goff, S. Maron, I. Maurin, F. Guillen, A. Garcia, T. Gacoin and J. P. Boilot, *J. Am. Chem. Soc.*, 2010, **132**, 10967–10969.
30 Q. Benito, X. F. Le Goff, S. Maron, A. Fargues, A. Garcia, C. Martineau, F. Taulelle, S. Kahlal, T. Gacoin, J. P. Boilot and S. Perruchas, *J. Am. Chem. Soc.*, 2014, **136**, 11311–11320.
31 A. Kobayashi, Y. Yoshida, M. Yoshida and M. Kato, *Chem.–Eur. J.*, 2018, **24**, 14750–14759.
32 G. N. Liu, L. Le Liu, Y. N. Chu, Y. Q. Sun, Z. W. Zhang and C. Li, *Eur. J. Inorg. Chem.*, 2015, **2015**, 478–487.
33 R. Meijboom, R. J. Bowen and S. J. Berners-Price, *Coord. Chem. Rev.*, 2009, **253**, 325–342.
34 C. R. Groom, I. J. Bruno, M. P. Lightfoot and S. C. Ward, *Acta Crystallogr., Sect. B: Struct. Sci., Cryst. Eng. Mater.*, 2016, **72**, 171–179.
35 P. S. Usama Fayyad and G. Piatetsky-Shapiro, *AI Magazine*, 1996, 37–54.
36 D. Hofmann and L. Kuleshova, *Data Mining in Crystallography*, 2010.
37 B. M. Jansen, *Angew Chem. Int. Ed. Eng*, 1987, **26**, 1098–1110.
38 P. Pyykkö, *Chem. Rev.*, 1997, **97**, 597–636.
39 D. L. Phillips, C. M. Che, H. L. King, Z. Mao and M. C. Tse, *Coord. Chem. Rev.*, 2005, **249**, 1476–1490.
40 P. Pyykkö, N. Runeberg and F. Mendizabal, *Chem.–Eur. J.*, 1997, **3**, 1451–1457.
41 A. Dedieu and R. Hoffmann, *J. Am. Chem. Soc.*, 1978, **100**, 2074–2079.
42 Y. Jiang, S. Alvarez and R. Hoffmann, *Inorg. Chem.*, 1985, **24**, 749–757.
43 C. Janiak and R. Hoffmann, *J. Am. Chem. Soc.*, 1990, **112**, 5924–5946.

44 P. K. Mehrotra and R. Hoffmann, *Inorg. Chem.*, 1978, **17**, 3913.
45 P. W. Atkins and R. S. Friedman, *Molecular Quantum Mechanics*, Oxford Univ. Press, 4th edn, 2005, DOI: **10.1002/bio.1290**.
46 K. Raghavachari and J. B. Anderson, *J. Phys. Chem.*, 1996, **100**, 12960–12973.
47 M. A. Omary, T. R. Webb, Z. Assefa, G. E. Shankle and H. H. Patterson, *Inorg. Chem.*, 1998, **37**, 1380–1386.
48 S. Dawn, S. R. Salpage, M. D. Smith, S. K. Sharma and L. S. Shimizu, *Inorg. Chem. Commun.*, 2012, **15**, 88–92.
49 D. Perreault, M. Drouin, A. Michel, V. M. Miskowski, W. P. Schaefer and P. D. Harvey, *Inorg. Chem.*, 1992, **31**, 695–702.
50 C. M. Che, M. C. Tse, M. C. W. Chan, K. K. Cheung, D. L. Phillips and K. H. Leung, *J. Am. Chem. Soc.*, 2000, **122**, 2464–2468.
51 P. D. Harvey, *Coord. Chem. Rev.*, 1996, **153**, 175–198.
52 D. Perreault, M. Drouin, A. Michel and P. D. Harvey, *Inorg. Chem.*, 1993, **32**, 1903–1912.
53 A. H. Johnstone, *J. Chem. Technol. Biotechnol.*, 2007, **50**, 294–295.
54 S. L. James, C. J. Adams, C. Bolm, D. Braga, P. Collier, T. Frišcic, F. Grepioni, K. D. M. Harris, G. Hyett, W. Jones, A. Krebs, J. Mack, L. Maini, A. G. Orpen, I. P. Parkin, W. C. Shearouse, J. W. Steed and D. C. Waddell, *Chem. Soc. Rev.*, 2012, **41**, 413–447.
55 D. Braga, F. Grepioni, L. Maini, P. P. Mazzeo and B. Ventura, *New J. Chem.*, 2011, **35**, 339–344.
56 L. Maini, D. Braga, P. P. Mazzeo and B. Ventura, *Dalton Trans.*, 2012, **41**, 531–539.
57 I. J. Bruno, J. C. Cole, P. R. Edgington, M. Kessler, C. F. Macrae, P. McCabe, J. Pearson and R. Taylor, *Acta Crystallogr., Sect. B: Struct. Sci.*, 2002, **58**, 389–397.
58 G. M. Sheldrick, *Acta Crystallogr., Sect. A: Found. Adv.*, 2015, **71**, 3–8.
59 R. Herbst-Irmer and G. M. Sheldrick, *Acta Crystallogr., Sect. B: Struct. Sci.*, 1998, **54**, 443–449.
60 A. A. Coelho, *J. Appl. Crystallogr.*, 2018, **51**, 210–218.
61 C. F. MacRae, I. Sovago, S. J. Cottrell, P. T. A. Galek, P. McCabe, E. Pidcock, M. Platings, G. P. Shields, J. S. Stevens, M. Towler and P. A. Wood, *J. Appl. Crystallogr.*, 2020, **53**, 226–235.
62 M. Che, J. C. Ve and E. J. Welzel, Characterization of Solid Materials and Heterogeneous Catalysts, 2012.
63 C. Jentoft, in *Advances in Catalysis*, Academic Press, 2009, vol. 52, pp. 129–211.
64 M. Abul Haj, C. B. Aakeröy and J. Desper, *New J. Chem.*, 2013, **37**, 204–211.
65 L. Maini, P. P. Mazzeo, F. Farinella, V. Fattori and D. Braga, *Faraday Discuss.*, 2014, **170**, 93–107.